Biol. Cybern. 74, 41–54 (1996)

Biological Cybernetics

© Springer-Verlag 1996

Coordination dynamics of trajectory formation

J. J. Buchanan [1], J. A. S. Kelso [1], A. Fuchs [1,2]

[1] Program in Complex Systems and Brain Sciences, Center for Complex Systems, Florida Atlantic University, PO Box 3091, Boca Raton, FL 33431-0991, USA
[2] Institut für Theoretische Physik und Synergetik, Universität Stuttgart, Pfaffenwaldring 57, D-70550 Stuttgart, Germany

Received: 24 February 1995/Accepted in revised form: 8 August 1995

Abstract. The present study aims to understand the neurally based coordination dynamics (multistability, loss of stability, transitions, etc.) of trajectory formation in a simple task. Six subjects produced two spatial patterns of coordination in the xy plane by alternating the abduction-adduction and flexion-extension motions of their right index finger. Each pattern was characterized by a unique temporal ratio between the x and y directions of motion: (1) a figure zero, a 1:1 temporal pattern; and (2) a figure eight, a 2:1 temporal pattern. The patterns were produced rhythmically and movement frequency was scaled across ten frequency plateaus, with ten cycles of motion per step. As movement frequency increased, switching from a figure eight to a figure zero was observed at critical cycling frequencies. The switch from pattern (2) to pattern (1) was identified in the spatial trajectory and power spectra of $x(t)$ and $y(t)$. En route to the transition, enhancement of fluctuations was observed in the Fourier amplitudes of $x(t)$ and $y(t)$, specifically at f_0 (the metronome frequency) and $2f_0$ (the first harmonic of f_0). Interestingly, there was no difference in the spatial variability of the two patterns. Overall, the data demonstrate that spatial patterns of coordination can be characterized in terms of the temporal relationship between the spatial components of the trajectory itself. We discuss the experimental findings in relation to other end-point planning and multijoint control strategies, as well as the much more general problem of temporal synchronization in many interlimb and intralimb coordination tasks.

1 Introduction

Moving the hand along a spatial path (trajectory), e.g., when reaching for an object, writing on a piece of paper or just doodling, requires the coordination of many neurons, muscles and joints. Compounding the problem of coordinating many individual degrees of freedom is the fact that without imposing any external constraints on a multijoint limb such as the arm, there is a large degree of redundancy. That is to say, in a multijoint limb of three or more degrees of freedom there are many joint angle combinations that may satisfy the same end-point position or end-point path. Also, the same end-point trajectory may be traversed with many joint angular combinations. This is without consideration of the numerous muscle combinations that are available. From a computational point of the view, the problem of trajectory formation is 'ill-posed' and has typically been treated as a problem of solving the inverse kinematics and inverse dynamics relation between end-point, joint angles and joint torques. Even though an infinite number of solutions exist, an extensive amount of experimental work has demonstrated that only a few possibilities are actually realized. For example, in pointing and reaching tasks the path of the end effector is either straight or slightly curved (e.g., Morasso 1981; Abend et al. 1982; Atkeson and Hollerbach 1985) and the velocity profile bell-shaped (Kelso et al. 1979; Flash and Hogan 1985). Other work on discrete pointing tasks and rhythmical drawing tasks has shown the joints are highly constrained in terms of their temporal relations (Soechting and Lacquaniti 1981; Lacquaniti and Soechting 1982; Soechting et al. 1986). Finding invariant features at different levels has created a debate as to whether end-point control is planned in terms of joint angle or end-effector coordinates (Flash and Hogan 1985; Soechting 1989; Soechting and Terzuolo 1990; Bizzi et al. 1992). As a result, a variety of geometric (Morasso and Mussa-Ivaldi 1982; Morasso 1983), kinematic (Abend et al. 1982; Flash and Hogan 1985; Soechting and Terzuolo 1986), biomechanical (Uno et al. 1989; Bizzi et al. 1992) and task-dynamical (Saltzman and Kelso, 1987) models of trajectory formation have been developed in favor of one position or the other.

Although an understanding of how end-point coordinates are mapped on to joint angles and muscle properties is very important, here we do not seek a specific type of mapping or concern ourselves with the inverse kinematics or dynamics problem. Instead, we focus on an

Correspondence to: J. A. S. Kelso

examination of two important functional properties of neuromotor coordination, i.e., multistability and pattern switching, that have received little attention in the context of the problem of trajectory formation. To address these features, the system's behavior must be examined in its nonlinear range where coordinative patterns arise and undergo change. The reason is that it is near *critical points* or *instabilities* that the system's relevant coordination variables (order parameters or collective variables) can be identified (Haken 1983; Kelso and Schöner 1987; Schöner and Kelso 1988a). Previous work has shown that multistability and pattern switching may be understood by studying transitions between temporally defined coordination patterns, e.g., in interlimb (Kelso 1981, 1984; Haken et al. 1985; Schmidt et al. 1991), intralimb (Kelso et al. 1991a; Buchanan and Kelso 1993) and perception-action (Kelso et al. 1990; Wimmers et al. 1992) tasks. Switching occurs when the system is driven to a critical value of a control parameter, e.g., frequency of motion, spatial orientation. At these critical points or instabilities, the components of a pattern must be disassembled and reassembled into another pattern. Variables that undergo qualitative change within this switching region, e.g., the relative phase between the fingers, hands, legs or joints of an arm, are taken to be task-specific collective variables. When transitions between movement patterns are accompanied by loss of stability, coordinative change is said to be self-organized (e.g., Haken 1983; Kelso 1984, 1995; Schöner and Kelso 1988a). Key signatures of loss of stability are *enhancement of fluctuations* (Kelso and Scholz 1985; Kelso et al. 1986; Schöner et al. 1986; Schmidt et al. 1990) and *critical slowing down* (Scholz et al. 1987; Scholz and Kelso 1989; Buchanan and Kelso 1993) in the collective variable as the transition region is approached. Once task-specific order parameters are identified, the coordinative patterns are then mapped onto attractors of a low-dimensional nonlinear dynamical system (e.g., Kelso and Schöner 1987), and the *order parameter* dynamics (equations of motion) are taken to represent the dynamics of the coordinative patterns. Identifying the system's relevant task-specific coordination variables provides an opportunity to establish relations between levels, i.e., by deriving the order parameter's equation of motion from the interactions of the individual components (see, e.g., Haken et al. 1985; Kelso and Scholz 1985; Schöner and Kelso 1988a, b).

Here, we treat the problem of trajectory formation as a self-organized pattern formation process, in order to determine whether spontaneous transitions among spatial coordination patterns occur and, if so, the form that they take. Some patterns, for example, may be more or less stable than others. Does pattern switching occur and is it due to an instability? What quantities (order parameters) best describe the stability properties of spatial patterns? To examine these questions, we study the two-dimensional (x, y) trajectories of an end effector (the right index finger) under parametric changes in movement frequency. Whereas much of the aforementioned work on end-effector trajectories has focused on the geometric and kinematic aspects of the end-effector trajectory or joint angle relations, here we focus on the underlying *temporal* ordering between the components of the generated *spatial* pattern, that is, between motion in the x and y directions on the frontal plane. We show that collective variables of the patterns may be defined in terms of the amplitudes and phases of the Fourier coefficients of x and y motion.

2 Experimental methods

2.1 Experimental apparatus

The x, y, z displacement of two infrared light-emitting diodes (IREDs) attached to the right index finger were recorded with the Optotrak 3D Motion Analysis System. This camera system consists of three one-dimensional sensors (anamorphic lenses) mounted in a single unit. Each sensor has a $34° \times 34°$ field of view and the sensor array has a precalibrated factory resolution of 0.1 mm in the x and y directions and 0.15 mm in the z direction at a distance of 2.5 m. The camera was mounted horizontally (at a level slightly above the subject's waist) and subjects were seated 2 m from the camera's center sensor. A specially designed hand apparatus was used to constrain motion of the forearm, wrist, thumb, and nonparticipating digits of the right arm. The forearm and wrist were secured in a Plastiform mold with the use of two Velcro straps (one over the forearm and the other just posterior to the wrist). The subject grasped a horizontal bar placed directly under the palm and extended the right index finger over the bar perpendicular to the camera. One IRED was attached to an aluminium sleeve that slid over the right index finger tip up to the second phalangeal joint and another IRED was mounted on the second metacarpophalangeal joint. A computer-generated auditory metronome (a 30-ms square-wave pulse output by a Mac II) was output over a loudspeaker mounted to the left of the subject. The IRED signals were monitored, recorded and stored on a Dell (466/M) PC, and the metronome signal was recorded with the Optotrak/Odau (analog to digital) device and also stored on the Dell PC. Both the IRED and metronome signals were recorded at a sampling frequency of 100 Hz.

2.2 Task and procedures

Six right-handed subjects (1 woman and 5 men), 24–45 years of age, participated in this experiment. None of the subjects reported any physiological impairment of the right arm. Subjects were required to coordinate the simultaneous flexion-extension and abduction-adduction of the right index finger so as to produce two spatial patterns of coordination: (1) a figure eight and (2) a figure zero. Idealized versions of these patterns are shown in Fig. 1A (zero) and Fig. 1B (eight). Five practice trials lasting a total of 1 min and paced at a movement frequency of 1.0 Hz were used to familiarize the subjects with the patterns and signalling system. A total of ten experimental trials of each pattern (in alternating blocks of five trials each) were performed following practice of the spatial patterns. Movement frequency was scaled in

the experimental trials from an initial frequency of 0.8 Hz to a final frequency of 1.7 Hz in 0.1-Hz steps, with ten cycles of motion per step. Each trial lasted approximately 80 s and the entire session approximately 1 h. The subjects were instructed to produce one complete cycle of motion, an entire figure eight or zero, for each beat of the metronome. The subjects were not required to synchronize any given reference point of the pattern with the metronome, e.g., the top or bottom of either pattern. Subjects were also instructed to maintain the initial spatial pattern of coordination for as long as possible and, should they feel the pattern begin to change, 'not to intervene', but to adopt the most comfortable spatial pattern of coordination between the horizontal (abduction/adduction) and vertical (flexion/extension) components of motion without losing time with the metronome.

3 Data analysis and results

3.1 Subject grouping

In general, the data from the figure zero trials were similar for all six subjects. However, the data generated in the figure eight trials prompted us to define the following subject groupings. Spontaneous switching from a figure eight to zero pattern was observed in the data of S1, S3 and S4 on all ten trials. We will focus on these three subjects in Sects. 3.4–3.6. Pattern switching was observed in the figure eight trials of S2 but not from an eight to zero. Instead, this subject switched from a figure eight to a different spatially and temporally defined pattern in xy-space. The data of S2 will be presented in detail in Sect. 4.1 and compared with the data of S1, S3 and S4. The behavior of the remaining two subjects, S5 and S6, departed dramatically from that of the other four subjects in the figure eight trials and their data will be discussed in Sect. 4.2.

3.2 Accuracy of tracking

To examine the effects of increasing cycling frequency on spatial patterns of coordination, we first show that subjects tracked the required metronome frequency with accuracy. Using a peak-picking algorithm, peak-to-peak cycle durations were calculated from $y(t)$ by taking the time difference between the peak at t_{n+1} and the peak at t_n for each cycle. The individual cycle durations (ten per plateau) were averaged within a plateau by trial to produce a mean cycle duration (T) as a function of required frequency, f_r. The actual plateau cycling frequency is, then, $f_p = 1/T$. A regression of f_p on f_r for each subject by condition produced r^2 values $\geqslant 0.9$, except for S6 in the figure eight condition ($r^2 = 0.84$). Overall, the high r^2 values indicate that the subjects paced quite well with the metronome.

3.3 Basic patterns: spatial trajectories and Fourier decomposition

Idealized version of the spatial patterns constructed from harmonic oscillations are plotted in Fig. 1A (zero) and Fig. 1B (eight). The corresponding x and y time series for one cycle of motion are plotted in Fig. 1C (zero) and Fig. 1D (eight), and representative line spectra plots of

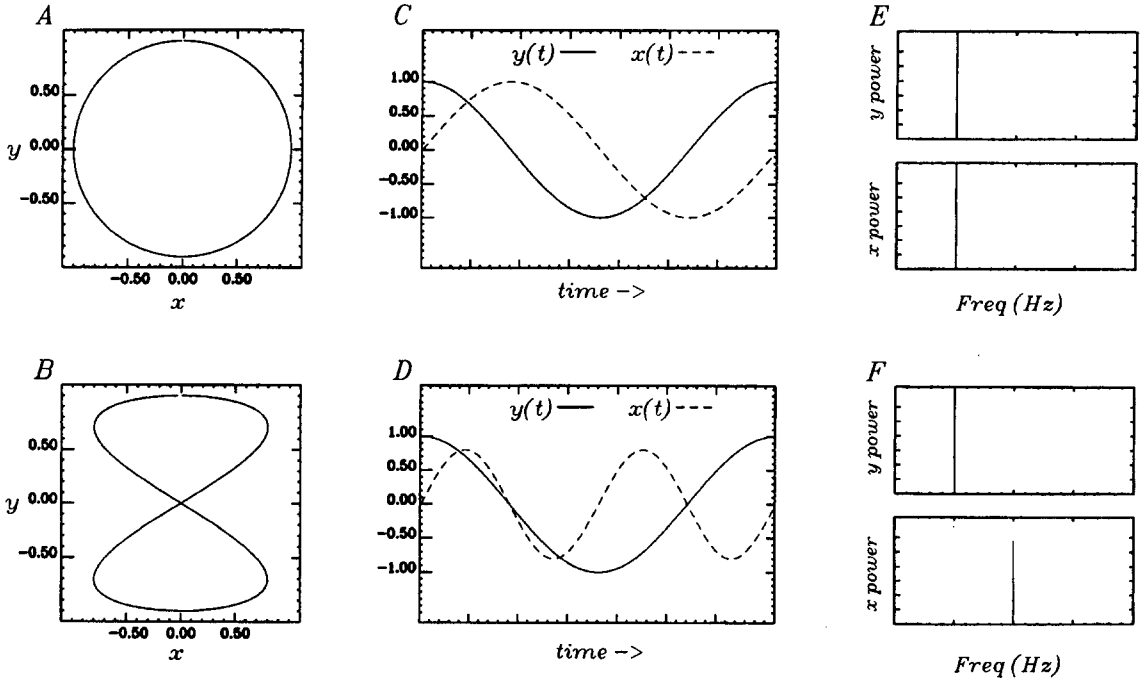

Fig. 1A–F. Depicted in **A** (eight) and **B** (zero) are idealized examples of the required patterns constructed form sinusoidal waveforms. The patterns in **A** and **B** are decomposed into their respective x and y time series in **C** and **D**. The power spectra for these single cycles are shown in **E** and **F**

$x(t)$ and $y(t)$ (for any frequency of motion) are plotted in Fig. 1E (zero) and Fig. 1F (eight). The line spectra show that each spatial pattern may be uniquely defined in terms of a specific temporal relationship between x and y motion: the zero pattern, a 1:1 temporal ratio (Fig. 1E); and the eight pattern, a 2:1 temporal ratio (Fig. 1F).

How well did the subjects' observed behavior comply with these ideal cases? Two complete trials for a figure zero and eight, plotted as a function of required cycling frequency, are shown in Fig. 2A and B, respectively. The 1:1 frequency ratio characterizing the zero pattern is evident in the spectral plots (Fig. 2A, rows 2 and 3). The alignment of the lone peak in the power spectra with the vertical dashed line demonstrates that this subject (S3) paced quite well with the metronome for all required frequencies. The behavior displayed in this trial is typical of all the figure zero trials for all subjects. The picture for the figure eight pattern is quite different. As seen in the superposition of $x(t)$ and $y(t)$ in Fig. 2B, the figure eight pattern is maintained through a required cycling frequency of 1.1 Hz, and then switches to the figure zero pattern around 1.2 Hz. This change in spatial pattern is reflected nicely in the spectral plots. Before the transition, there is a dominant peak in the x direction at twice the required frequency, and in the y direction there is a single peak at the required cycling frequency. After the transition, only single peaks at the required frequency are present in the spectral plots. This shift in temporal pattern from a 2:1 to 1:1 frequency ratio in xy-space reflects the change observed in the spatial trajectory. Also, notice that the shape of the figure zero in Fig. 2B is similar to the zero in Fig. 2A for the higher cycling frequencies. In general, the behavior portrayed in this figure eight trial is representative of the behavior of S1, S3 and S4. For these subjects, most of the observed transitions occurred between frequencies of 1.2 and 1.4 Hz.

The above description demonstrates that spatial patterns of coordination may be described in terms of the temporal pattern between the spatial components of the

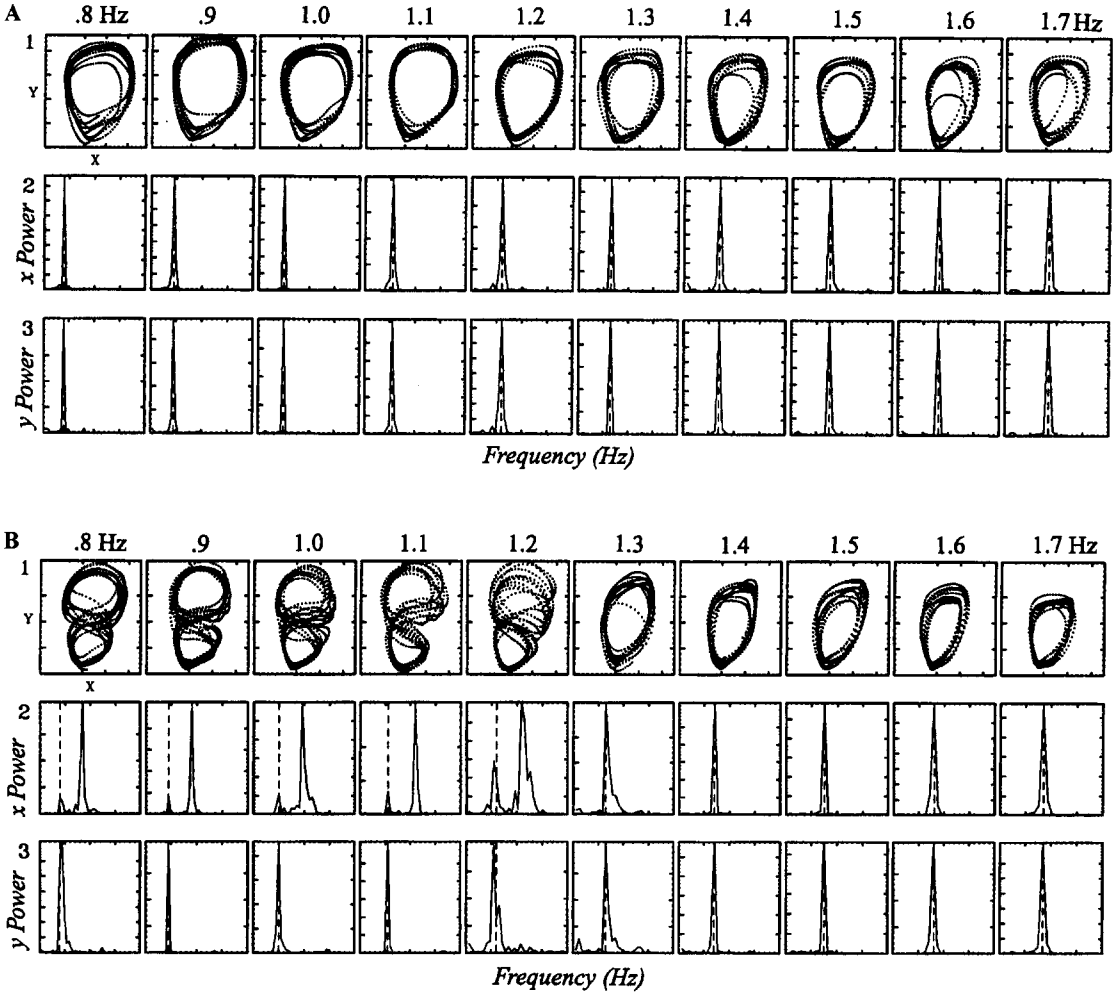

Fig. 2A, B. Complete trials from S3 for a figure zero (**A**) and a figure eight (**B**) are plotted as a function of required frequency. The raw spatial trajectories produced by the superposition of $x(t)$ and $y(t)$ have been reproduced in the *top row*. In the *second* and *third rows*, the corresponding power spectra for $x(t)$ and $y(t)$ have been plotted, respectively. The *vertical dashed line* in the power spectra plots in rows 2 (x spectrum) and 3 (y spectrum) corresponds to the metronome driving frequency

trajectory, in this case motion in the x and y directions. These results are in good agreement with the idealized cases. Spatial transitions can be characterized as a spontaneous switch in the temporal ordering of the spatial components. Next, we show that the transition from the figure eight to zero pattern resulted from a loss of stability in the 2:1 ratio between x and y. Both the direction of the transition and fluctuation enhancement are predicted from theoretical considerations regarding 2:1 to 1:1 transitions in coupled nonlinear oscillators (see Discussion).

3.4 Transitions in Fourier coefficients: loss of stability

In this section, we show that the spatial transition from a figure eight to zero resulted from a loss of stability in the temporal ratio between the x and y spatial components of the end effector. Pattern stability is assessed through an analysis of the Fourier coefficients of $x(t)$ and $y(t)$. Any significant increases in the variability of these coefficients before the transition will be taken as evidence for enhancement of fluctuations, a signature of loss of stability and impending behavioral change (e.g., Kelso and Scholz 1985; Kelso et al. 1986). Since subjects S1, S3 and S4 tracked the metronome accurately, we felt it appropriate to increase the resolution of our temporal measure in order to test for critical fluctuations. Thus we performed an FFT on $x(t)$ and $y(t)$ on a cycle-by-cycle basis (instead of by frequency plateau: see Fig. 2):

$$x(n\omega_T) = \frac{1}{T}\int_0^T x(t)e^{-in\omega_T t}\,dt \tag{1}$$

$$y(n\omega_T) = \frac{1}{T}\int_0^T y(t)e^{-in\omega_T t}\,dt \tag{2}$$

where T is the required cycle duration as a function of the metronome frequency $n\omega_T$ and $\omega_T = 2\pi/T$, the fundamental frequency. Next we normalized the power of the individual cycle coefficients $X^{(1)}$, $Y^{(1)}$, and $X^{(2)}$, $Y^{(2)}$ corresponding to f_0 and $2f_0$, respectively, to the range 0 to 1:

$$x(\omega_{1,2}) = |C_x(\omega_{1,2})|^2/E_x \tag{3}$$

$$y(\omega_{1,2}) = |C_y(\omega_{1,2})|^2/E_y \tag{4}$$

with

$$E_x = \sum_{k=1}^{7} |C_x(\omega_K)|^2/n \tag{5}$$

$$E_y = \sum_{k=1}^{7} |C_y(\omega_K)|^2/n \tag{6}$$

where $C(\omega_K)$ indicates complex coefficients, n is the number of data points within the metronome period for a given plateau, and k corresponds to the first seven coefficients computed from (1) and (2). To arrive at a mean power value for each plateau, we averaged the individual cycle values of $X^{(1,2)}$ and $Y^{(1,2)}$ within each individual trial:

$$\bar{X}_p^{(1,2)} = \sum_{p=1}^{P}\sum_{n=1}^{N} X_{pn}^{(1,2)}/N \tag{7}$$

$$\bar{Y}_p^{(1,2)} = \sum_{p=1}^{P}\sum_{n=1}^{N} Y_{pn}^{(1,2)}/N \tag{8}$$

where P is the number of plateaus (i.e., 10) and N the number of cycles in each plateau. Cycle one on plateau one is considered a startup or transient cycle and therefore dropped from the analysis. Thus N is 9 for plateau one and 10 for all the other plateaus.

In the case of the figure zero, the values of $\bar{X}_p^{(1,2)}$ $\bar{Y}_p^{(1,2)}$ were averaged (across subjects) as a function of cycling frequency, and for the figure eight, the values of $\bar{X}_p^{(1,2)}$ $\bar{Y}_p^{(1,2)}$ were aligned to the transition plateau and averaged backwards and forwards (across subjects) from this point. This produced a total of five pre-transition and four post-transition plateaus in the figure eight data. Plotted in Fig. 3A–D are the resulting group means of $\bar{X}_p^{(1,2)}$ $\bar{Y}_p^{(1,2)}$ and their standard deviations for the figure eight and zero. The group mean and standard deviations were compared statistically. The pre-transition figure eight data were compared with the first five frequency plateaus of the figure zero (0.8–1.2 Hz) in a 2 condition (eight vs zero) × 5 plateau (pre-tran) ANOVA, and the post-transition figure eight data were compared with the last four frequency plateaus of the figure zero (1.4–1.7 Hz) in a 2 condition × 4 plateau (post-tran) ANOVA.

For the figure zero (Fig. 3A, C), the values of $X^{(1)}$ and $Y^{(1)}$ remain near 0.95 across all frequencies,while the values of $X^{(2)}$ and $Y^{(2)}$ remain near 0.04. The picture is quite different for the figure eight (Fig. 3B, D). Before the transition (pre-transition plateaus 5 through 1 on the abscissa), the value of $X^{(1)}$ is around 0.25 and $Y^{(1)}$ around 0.86, while the value of $X^{(2)}$ is around 0.68 and $Y^{(2)}$ around 0.1. The statistical analyses confirm that the power in the pre-transition values of $X^{(1,2)}$ and $Y^{(1,2)}$ for the figure eight is significantly different from those of the figure zero across the first five frequency plateaus (0.8–1.2 Hz), $Fs(1, 336) > 125.6$, $ps < 0.01$. These differences confirm our earlier predictions based on the sinusoidal representation of the patterns (Fig. 1) and the power spectra plots shown in Fig. 2. These figures indicate that the power in the x-direction of the figure eight should be concentrated in $X^{(2)}$, while the power in the x-direction of the figure zero should be concentrated in $X^{(1)}$. As for the y-direction, our representation suggests that if any difference occurs between patterns it should be small. Thus it is not surprising that the order of greatest to least statistical significance is as follows: $X^{(1)}$, $X^{(2)}$, $Y^{(1)}$, $Y^{(2)}$. Differences between the two patterns are also evident in the mean variability of the Fourier amplitudes. As seen in Fig. 3A and C, the variability of $X^{(1,2)}$ and $Y^{(1,2)}$ for the figure zero is small (< 0.05) and constant across all cycling frequencies. The variability of $Y^{(1,2)}$ and especially $X^{(1,2)}$ for the figure eight (Fig. 3B, D) is much larger across the pre-transition plateaus than is the case for the figure zero for all frequencies, and increases

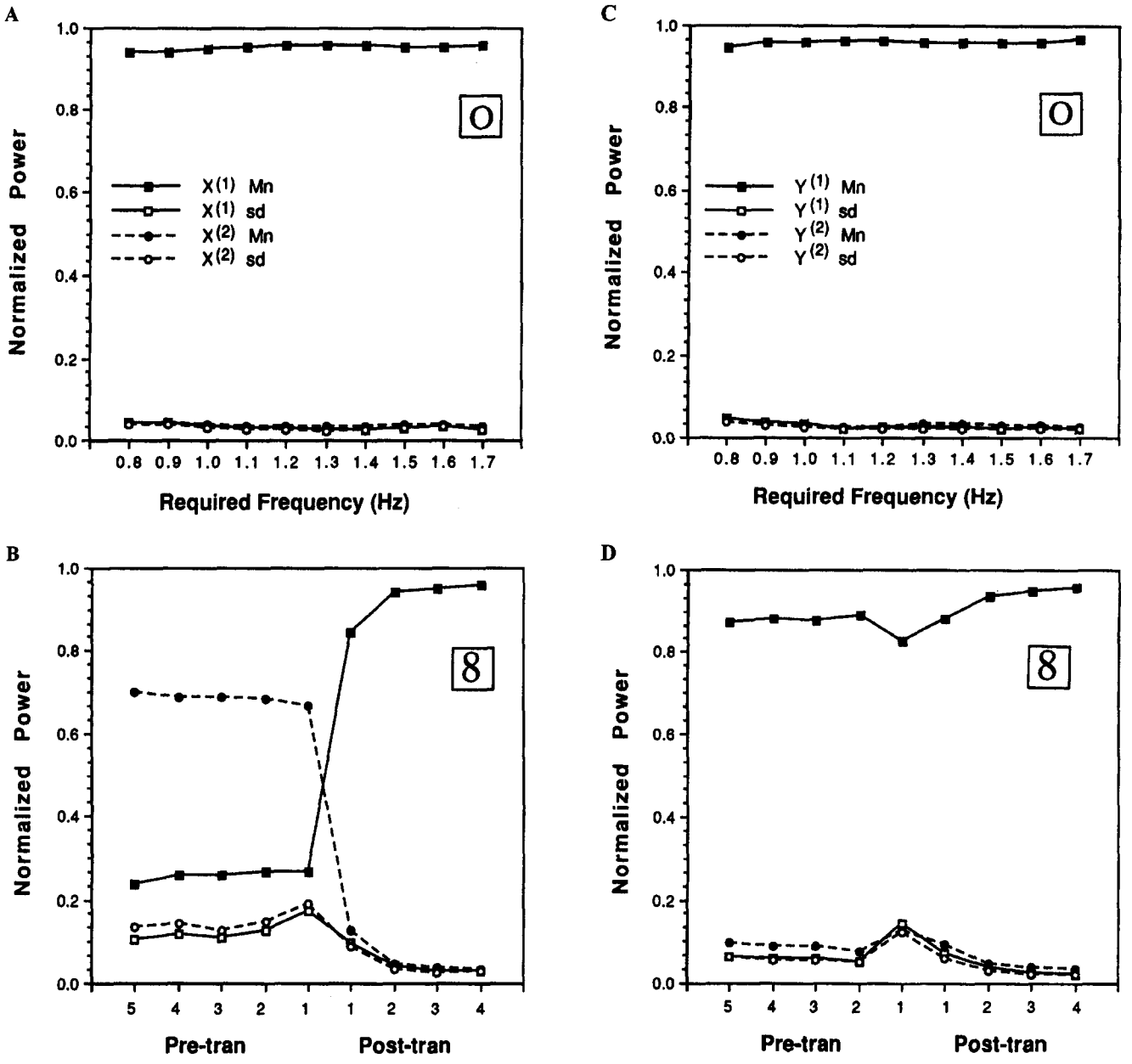

Fig. 3A–D. Means (*Mn*) and standard deviations (*sd*) of $X^{(1,2)}$ and $Y^{(1,2)}$ for the figure zero are plotted in A and C, respectively, as a function of required frequency. The means and standard deviations of $X^{(1,2)}$ and $Y^{(1,2)}$ for the figure eight are plotted in B and D, respectively, as a function of pre-transition and post-transition plateaus

just before the switch between patterns. Statistically, the standard deviations of all four coefficients for the pre-transition figure eight are significantly larger than those of the figure zero across the first five frequency plateaus: $Fs(1, 336) > 64.7$, $ps < 0.01$. Also, the variability of the figure eight just before the transition is significantly larger than the variability in the other pre-transition positions: $Fs(5, 336) > 3.6$, $ps < 0.01$. After the transition, the means and standard deviations of $X^{(1,2)}$ and $Y^{(1,2)}$ for the post-transition figure eight (plateaus 1 through 4 on the abscissa), now a figure zero, take on values indistinguishable from the figure zero for frequency values of 1.4–1.7 Hz. This is quite evident in the change in power of $X^{(1)}$ and $X^{(2)}$ following the transition (Fig. 3B). Statistical analyses of the post-transition means and standard deviations reveal some small differences between the two figure zero patterns: means, $Fs(1, 259) > 14.6$, $ps < 0.01$; and standard deviations, $Fs(1, 259) > 10.6$, $ps < 0.01$. Simple main effect tests indicated that these effects result from a difference in the patterns on the first post-transition plateau in the figure eight trials (now a figure zero) and the figure zero pattern at 1.4 Hz. After this plateau, there are no significant differences between the two zero patterns. As with the pre-transition results, the above analyses of the post-transition means conform quite well with our hypotheses regarding the distribution

and change in distribution of the power in the patterns as represented in Figs. 1 and 2.

3.5 *Fourier phases*

The switch from a figure eight to zero pattern can also be seen in the phases $\phi^{(1,2)}$ of $X^{(1,2)}$. To enhance this picture, following the cycle-by-cycle FFT performed on $x(t)$ and $y(t)$ in (1) and (2), we shifted $\theta^{(1)}$ (the phase of $Y^{(1)}$) to zero and the phases $\phi^{(1,2)}$ were shifted an equivalent amount. The cycle-by-cycle phase of $\phi^{(1,2)}$ following this shift were plotted as distributions to qualitatively compare the figure eight and zero patterns.

For the figure zero, the phase distributions plotted as a function of cycling frequency (for all six subjects) had peaks centered around $\pm$ 90° (depending on the direction of motion, clockwise or counterclockwise) for $\phi^{(1)}$ with the distribution of $\phi^{(2)}$ spread over the interval $-$ 180° to 180° (not shown). As with the amplitudes, the picture for the figure eight is quite different. Plotted in Fig. 4 as a function of pre- and post-transition plateaus are histograms of $\phi^{(1)}$ and $\phi^{(2)}$ for the figure eight. Before the transition, the distribution of $\phi^{(2)}$ (Fig. 4A) is centered around 90° and the distribution of $\phi^{(1)}$ (Fig. 4B) is spread over the interval $-$ 180° to 180°. After the transition, the distribution of $\phi^{(2)}$ broadens and two well-defined peaks centered around $\pm$ 90° arise in $\phi^{(1)}$. Positive and negative peaks are observed because S1 and S4 produced figure zeros in a counterclockwise direction after the transition and S3 (and S4 in two trials) produced figure zeros in a clockwise direction. These changes in the distributions of $\phi^{(1)}$ and $\phi^{(2)}$ correspond well with the switch in power observed between $X^{(1)}$ and $X^{(2)}$ after the transition (Fig. 3B). The transition from a figure eight to zero may be characterized as a switch from a 2:1 to 1:1 temporal pattern, with a phase difference near $\pm$ 90° between the main Fourier coefficients of $x(t)$ and $y(t)$.

3.6 *Spatial variability*

In this section, we present an analysis of the spatial properties of the trajectories themselves. Emphasis is placed on examining the spatial variability of the patterns in xy-space and how such variability may relate to the observed temporal variability reported above. This analysis involved deriving a mean spatial pattern for each frequency plateau within a trial for each subject. First, an FFT was performed on $x(t)$ and $y(t)$ on a cycle-by-cycle basis [see (1) and (2)]. Second, the phase $\phi^{(i)}$ and $\theta^{(i)}$ of $X^{(i)}$ and $Y^{(i)}$, respectively, were shifted by using $\theta^{(1)}$ as a reference for all $\phi^{(i)}$ and $\theta^{(i)}$ when $X^{(i)}$ and $Y^{(i)}$ were > 0. Following the shift in $\phi^{(i)}$ and $\theta^{(i)}$, the individual $x(t)$ and $y(t)$ cycle traces were reconstructed. In Fig. 5, we have plotted the original ($x(t)$, row 1 and $y(t)$, row 3) and reconstructed cycle traces ($x(t)$, row 2 and $y(t)$, row 4) for a complete trial of a zero (Fig. 5A) and eight (Fig. 5B) pattern for S1. The discontinuities in the reconstructed time series arise because the original signal is not purely periodic. However, in general, the reconstructed time series corresponded quite well with the original cycles.

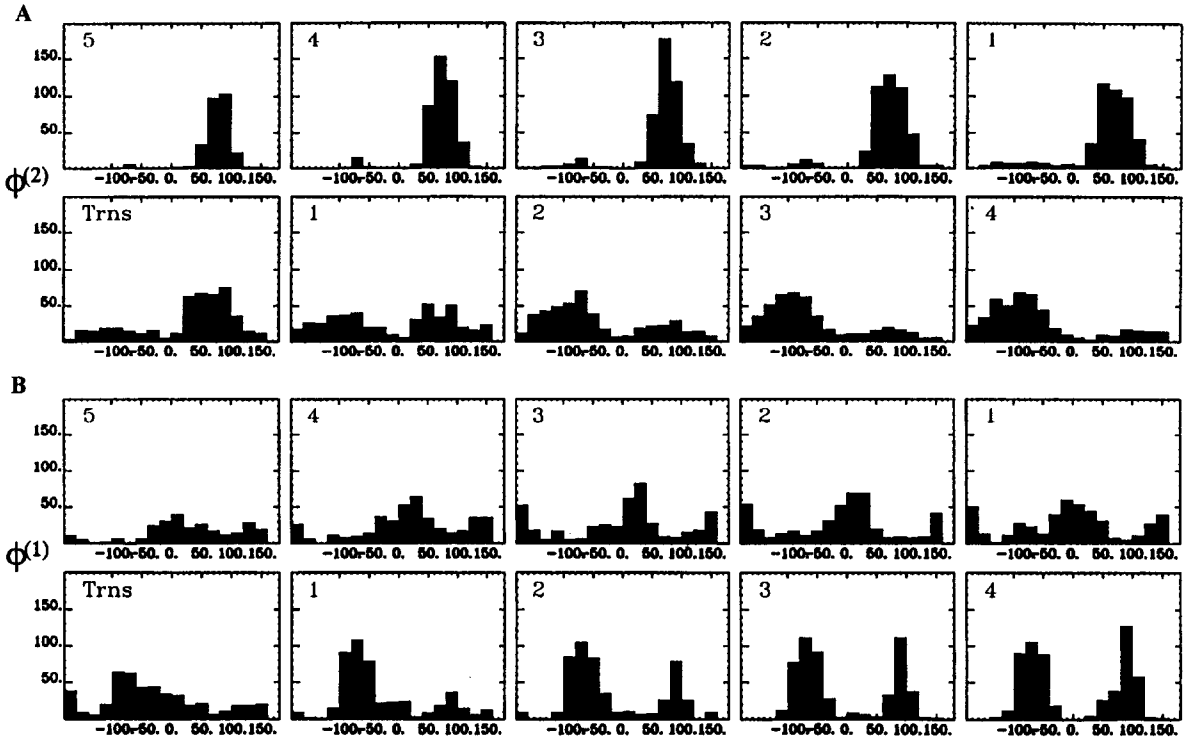

Fig. 4A, B. The distribution of $\phi^{(2)}$ and $\phi^{(1)}$ for S1, S3 and S4 are plotted in **A** and **B**, respectively, as a function of alignment to the transition plateau. The window size of the distributions is 18°

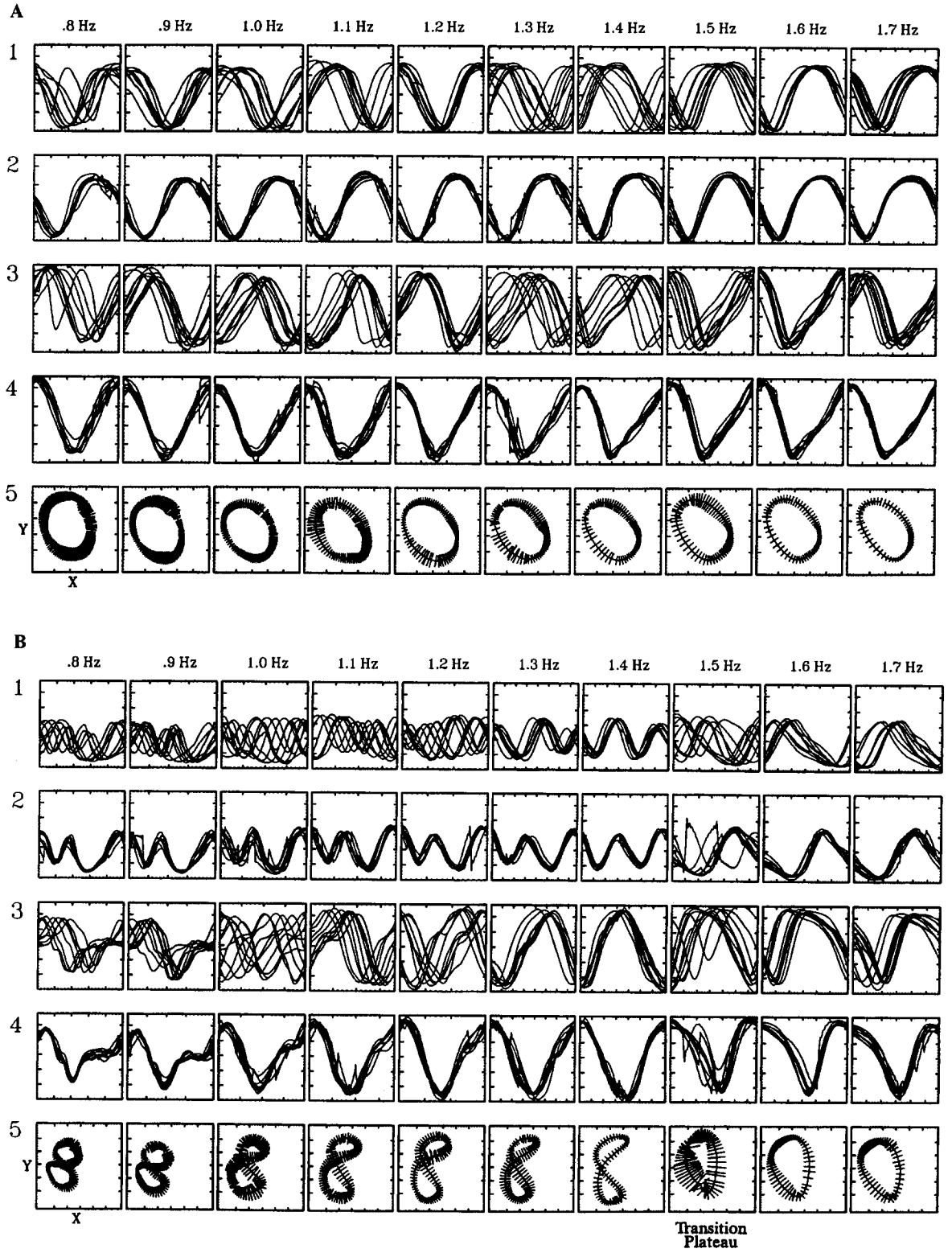

Fig. 5A, B. Individual cycle time series for x (*row 1*) and y (*row 3*) are plotted as a function of required frequency for a figure zero (**A**) and a figure eight (**B**). The reconstructed time series of x and y are plotted in *row 2* and *4*. The superposition of the average x and y time series produces the average spatial pattern shown in *row 5*. The spatial variability, S_{sd}, of the pattern is plotted as the variability band around the figures

After reconstructing the cycles, we averaged across the individual data points individually for each subject, x_i and y_i, for all cycles in the plateau to create a mean trajectory of motion in the x and y directions:

$$\bar{X}_n = \sum_{n=1}^{N} \sum_{c=1}^{C} x_{nc}/C \tag{9}$$

$$\bar{Y}_n = \sum_{n=1}^{N} \sum_{c=1}^{C} y_{nc}/C \tag{10}$$

where N is the number of data points in a metronome cycle and C the number of cycles in a plateau. Next we computed spatial variability, S_{var}, for each $(\bar{X}_n, \bar{Y}_n)$ pair in a plateau:

$$S_{\text{var}} = \sum_{n=1}^{N} \sum_{c=1}^{C} (\bar{X}_n - x_{nc})^2/C + (\bar{Y}_n - y_{nc})^2/C \tag{11}$$

and

$$S_{\text{sd}} = \sqrt{S_{\text{var}}} \tag{12}$$

where N is the number of data points in each cycle of a plateau and C the number of cycles in each plateau. In row 5 of Fig. 5A and B, the superposition of the $\bar{X}_n$, $\bar{Y}_n$ pairs produce a plot of the averaged trace for the spatial pattern as a function of required frequency. The variability of the pattern is represented by plotting the values of S_{sd} as lines orthogonal to the averaged trajectory.

The mean trajectory of the figure zero plotted in Fig. 5A maintains its shape as frequency increases. Spatial variability even tends to decrease with frequency. This is typical of all subjects for the figure zero. The figure eight more or less maintains its shape across frequency plateaus before the transition plateau (1.5 Hz) at least, in this case, with some indication that its variability changes as the transition region is approached. To examine this possibility, we computed a mean S_{sd} for each plateau by trial. These averaged values were treated as a measure of mean spatial variability of the patterns. The averaged values (across subjects) of S_{sd} are plotted as a function of cycling frequency for the figure zero in Fig. 6A. For the figure eight, we aligned the values of S_{sd} to the transition plateau and averaged backwards and forwards from this point; these values are plotted in Fig. 6B. This produced a total of five pre-transition and four post-transition plateaus in the figure eight data. The figure eight and zero S_{sd} values were compared statistically. The pre-transition data from the figure eight trials were compared with the first five frequency plateaus of the figure zero trials (0.8–1.2 Hz) in a 2 condition (eight vs zero) × 5 plateau (pre-tran) ANOVA. The post-transition data from the figure eight trials were compared with the last four frequency plateaus of the figure zero (1.4–1.7 Hz) in a 2 condition × 4 plateau (post-tran) ANOVA. Statistically, there is no difference in spatial variability between the figure zero and pre-transition figure eight: $F(1,279) = 1.0$, $p > 0.2$. This result seems slightly counterintuitive on the basis of an initial inspection of the data plotted in Fig. 6. To explore the spatial variability data further, we also tested the figure eight data against the zero pattern across frequency plateaus (0.9–1.3 Hz). This analysis also revealed no significant effect of pattern or plateau: $Fs < 2.0$, $p > 0.2$. After the transition, the spatial variability in the figure eight trials (now a figure zero) drops to the level of the zero pattern across frequencies 1.4–1.7 Hz, with no statistical difference in variability between the two figure zeros: $F(1,205) = 0.1$, $p > 0.8$. These results suggest that the temporal fluctuations

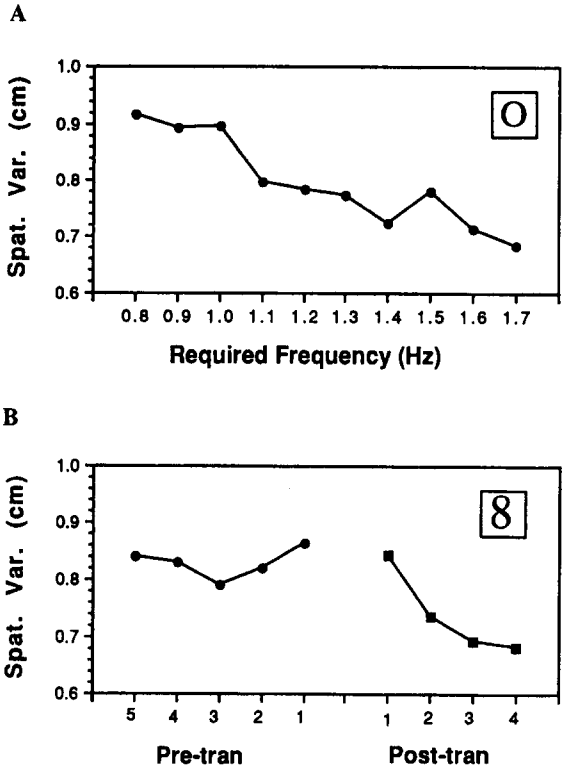

Fig. 6A, B. The mean spatial variability, i.e., the averaged S_{sd} values, collapsed across subjects for the figure zero are plotted as a function of required frequency in **A**. The mean spatial variability data for the figure eight is plotted as a function of pre-transition and post-transition plateau in **B**

before the transition are not mirrored in the actual spatial trajectory, which retains its cycle-to-cycle shape (see Fig. 5).

4 Other switching behavior

4.1 Temporally similar but spatially unique patterns

The previous results dealt with abrupt transitions from one spatial pattern to another. Here we show that the data of S2 exhibited a qualitative change in the initial figure eight pattern, but not from a figure eight to zero.

Plotted in Fig. 7 is a complete trial from the figure eight condition for S2. Initially, the spatial pattern resembles a figure eight. However, by plateau 2 (0.9 Hz) a qualitative change occurs as the bottom loop of the figure collapses and a new spatial pattern resembling the Greek letter ρ emerges across the mid to latter frequency plateaus. Such a clear qualitative change in spatial pattern occurred in seven of ten trials for S2, with the initial change occurring between 0.9 Hz and 1.3 Hz. The power spectra of $x(t)$ and $y(t)$ reveal two important temporal features of the pattern: (1) the subject paces with the metronome; and (2) the pattern is initially characterized by a 2:1 temporal ratio, but as the spatial form of the trajectory changes, a peak arises at the required frequency in the x spectrum. The change in spatial pattern is

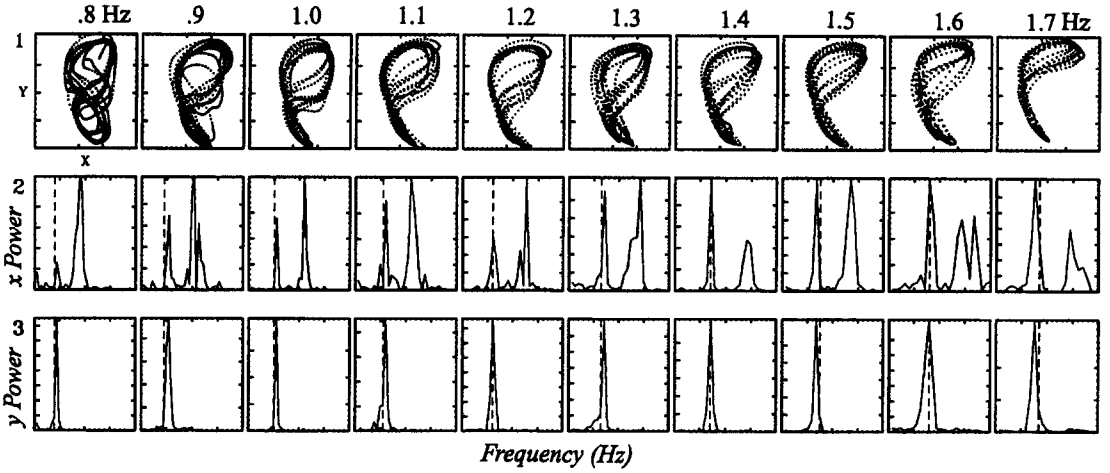

Fig. 7. A complete trial from the figure eight condition for S2 is plotted as a function of required frequency. The change in the spatial coordination pattern is evident in the superposition of $x(t)$ (*row 1*) and $y(t)$ (*row 2*) and is mirrored in the power spectra

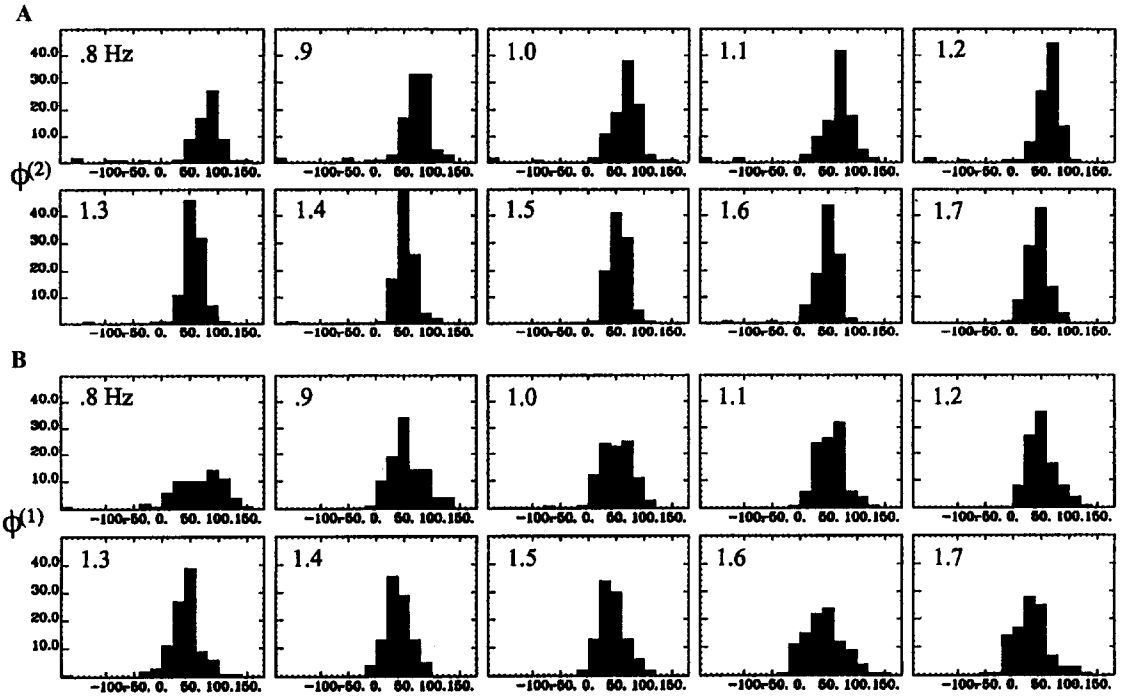

Fig. 8A, B. The distribution of $\phi^{(2)}$ and $\phi^{(1)}$ for S2 are plotted in A and B, respectively, as a function of required frequency for the seven trials in which the ρ pattern occurred

accompanied by an equivalent temporal change, and a temporal description of the pattern requires two frequency ratios: a 2:1 ratio between $X^{(2)}$ and $Y^{(1)}$ and 1:1 ratio between $X^{(1)}$ and $Y^{(1)}$.

These changes in the power spectra accompanying the emergence of this new pattern are reflected in the phase distribution of $\phi^{(1,2)}$ of $X^{(1,2)}$ following the same shifting procedure reported in Sect. 3.5. Plotted in Fig. 8 are the phase distributions of $\phi^{(2)}$ (Fig. 8A) and $\phi^{(1)}$ (Fig. 8B) for the figure eight trials (seven trials) as a function of required frequency. Two important differences exist between these distributions and those in Fig. 4. First, the $\phi^{(1)}$ distribution (Fig. 8B) is narrower for S2 compared with S1, S3 and S4 (Fig. 4B). Also, as the ρ pattern emerges at higher cycling frequencies, the peak in the distribution of $\phi^{(1)}$ shifts from near 70° to 40°. Second, the $\phi^{(2)}$ distribution is well defined for all frequency plateaus (compare Fig. 8A with Fig. 4A) and a shift in the peak of the distribution of $\phi^{(2)}$ from near 90° to 50° occurs as cycling frequency increases. These qualitative results suggest that the ρ pattern produced by S2 is a temporally more complex spatial pattern than either the figure eight or the figure zero. That is, the ρ pattern cannot be sufficiently described in terms of a single temporal ratio between x and y as shown in the ideal eight and zero patterns in Fig. 1 and the experimental examples shown in Fig. 2.

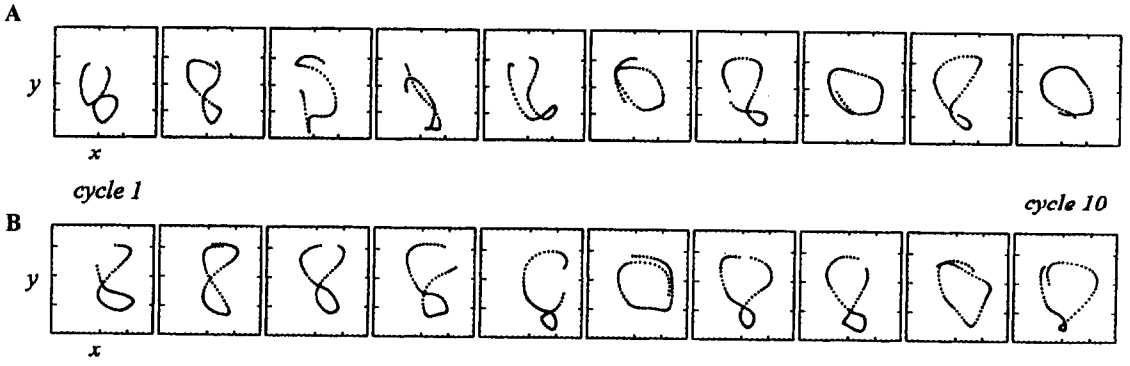

Fig. 9A, B. Two plateaus of data from two trials of S5 showing switching back and forth between a figure eight and zero are shown: **A** cycling frequency 1.4 Hz; **B** cycling frequency 1.5 Hz

4.2 Switching back and forth

The behavior of S5 and S6 in the figure eight condition did not conform to that of other subjects. Shown in Fig. 9 are two plateaus of data plotted as individual cycles from two trials for S5. This continual shifting back and forth between an eight and a zero was observed in the data of S5 and S6 in all ten trials for frequencies greater than 1.2 Hz. Since the figure eight pattern was temporally less stable than the figure zero (see Sect. 3.4), the eight pattern was not maintained for long following the first shift. Typically, the figure eight re-emerged for one to seven cycles following the switch to the zero pattern and then a shift back to a zero occurred for several cycles and then a switch back to the eight, and so on (Fig. 9B). Occasionally, a distorted pattern resembling neither an eight nor a zero was observed (Fig. 9A). This indicates that fluctuations were felt quite severely when an unstable pattern was maintained in proximity to a critical value of the control parameter (here the cycling frequency).

5 Discussion

The main hypothesis advanced in this paper is that the formation of spatial patterns of coordination (end-effector trajectories) is subject to coordination dynamics. Insights into how these dynamics are instantiated by the central nervous system may be revealed by studying the system in its nonlinear range of behavior where patterns arise and undergo change (Kelso 1984; Haken et al. 1985; Schöner and Kelso 1988a). Recently, several experiments examining rhythmic single limb multijoint (elbow and wrist) coordination (Kelso et al. 1991a; Buchanan and Kelso, 1993) and reaching and grasping (Kelso et al. 1994) have shown a strong relationship between the phase relation or timing among the joints and the end-effector trajectory. Although trajectory formation was not the focal point of such research, it nevertheless demonstrated that the formation of spatial patterns is intimately linked to the coordination among the components producing the trajectory. Specifically, these studies demonstrated that inter- and intralimb patterns of coordination and their stability can be understood in terms of dynamics, i.e., pattern switching, loss of stability, hysteresis, etc. In this experiment, we exploited the idea that pattern switching and concepts of stability may be used as a window into the problem of trajectory formation.

The choice of the spatial patterns studied was not based on their spatial or geometric characteristics, but instead on the temporal relation between the x and y components of the two-dimensional spatial pattern (Figs. 1, 3B). For low frequency values, both the figure eight and zero pattern were stably produced by all six subjects. As cycling frequency increased, transitions from a figure eight to zero occurred at critical cycling frequencies in three subjects, and this change in spatial pattern was easily identified in the superposition of $x(t)$ and $y(t)$ (Fig. 2). This switch in spatial pattern shows up clearly in the temporal ratio between the spatial components of the end-effector's trace, i.e., in the amplitudes and phases of the Fourier coefficients of $x(t)$ and $y(t)$. In the vicinity of the transition region, *enhancement of fluctuations* in the Fourier amplitudes was apparent in the data of S1, S3 and S4 (Fig. 3B, D). This observation supports the conclusion that the observed spatial transitions resulted from loss of stability, a key signature of self-organization. This is an important point in light of the data presented on the geometric variability of the patterns (Figs. 4, 5). Statistically, the spatial variability of the figure eight remained more or less constant and that of the figure zero tended to decrease with increasing frequency. As noted in Sect. 3.6, there is some indication that spatial variability in the figure eight increased immediately before the transition, although statistically speaking it was not significant. The exact nature of the temporal and spatial relationship, however, is somewhat ambiguous in our data. Further refinements of the experimental procedure may help to clarify the relation between the temporal and spatial aspects of end-point control. One way to shed some light on this would be to explore the figure eight pattern for long intervals in the vicinity of the critical frequency. Another way would be to utilize smaller time steps in the vicinity of the critical frequency. Such procedures may provide a more accurate measure of the relationship between temporal and spatially defined fluctuations in end-point trajectories. These spatial

averaging results when considered together with the temporal findings support the following conclusions. First, the spatial patterns studied in this task may be decomposed into relevant temporal variables that capture the essential features of the observed behavioral changes. Second, the temporal ratio (described in terms of the Fourier amplitudes) between spatial components is the relevant task-specific *collective variable* or *order parameter* capturing essential features of the system's coordination dynamics.

Even though the data of S2, S5 and S6 did not conform with those of the other subjects, their behavior remained consistent with expectations based on the synergetic or dynamic pattern strategy (Schöner and Kelso 1988a,b; Kelso and Schöner 1987), as well as a variety of results from other experiments. For example, although S2 switched from a figure eight to nonzero pattern, ρ, the shift is characterized by very systematic changes in both the Fourier amplitudes and phases of $x(t)$ and $y(t)$ (Figs. 7, 8). We expected that pattern switching would take the form of a 2:1 to 1:1 temporal patterning in xy-space based on the differential stability of frequency ratios (e.g. Kelso and DeGuzman 1988; Beek 1989; DeGuzman and Kelso 1991; Kelso et al. 1991b; Beek et al. 1992; Treffner and Turvey 1993). Of course, this does not exclude the possibility that other, more complex temporally defined spatial patterns may be more or less stable than our initial 2:1 pattern. For example, the ρ pattern produced by S2 is best characterized as a 1:1 and 2:1 temporal pattern between $X^{(1)}$ and $Y^{(1)}$ and $X^{(2)}$ and $Y^{(1)}$, respectively. The behavior of S2 raises the question of how a more complex temporal pattern obviates the need to switch between temporal patterns. One possibility is that other frequency components represent a marshalling of available temporal degrees of freedom to help stabilize the pattern. Some recent work on bimanual (Kelso et al. 1993) and single limb multijoint movements (Buchanan et al. 1994), has demonstrated that recruitment and suppression of kinematic degrees of freedom is a strategy that allows the system to adapt flexibly to changing environmental conditions without switching patterns. If temporal ratios are the relevant coordination variables in such end-point tasks, then the ability to recruit other frequency components (as S2 did) provides the system with another form of flexibility in addition to pattern switching. However, the serendipitous results associated with S2 only hint that temporal complexity may be defined in terms of the number of temporal ratios between the components. To define temporal complexity, it is necessary to study in more detail the switching relations between the patterns we studied, the ρ pattern, and other patterns.

The differences between S2 and the three transition subjects raises the issue of how equivalence classes of actions (cf. Greene 1972) are represented at more abstract levels. Two possibilities are suggested by the data: (1) equivalence classes are defined by the temporal ratio between components (1:1, 2:1, 3:2, etc.); or (2) they are defined by the number of prominent temporal ratios between components (1, 2, 3, etc.). In the former case, just the parameterization of the phase between two temporally coordinated components can produce different spatial patterns. For example, a figure C may be defined as a 2:1 temporal pattern in x, y with a 45° phase between x and y. By simply shifting the phase between temporal components, a variety of specific spatial trajectories can be produced. If this is the case, a spatial transition from an eight to a zero is a transition from one equivalence class to another. The latter possibility is suggested by the data of S2. In this case, a transition from an eight to a zero is a transition within an equivalence class of action that results from a loss of stability. Such an interpretation is in line with previous work on bimanual coordination (Kelso and Deguzman 1988; Treffner and Turvey 1993) that has shown that certain temporal relationships between interlimb components (e.g., 5:2, 4:3) are less stable than others (e.g., 3:1 or 1:1) (Kelso and DeGuzman 1988; Treffner and Turvey 1993). Pattern stability and the direction of pattern switching in these bimanual experiments has been linked to the width of the Arnol'd Tongues in the phase attractive circle map (DeGuzman and Kelso 1991, 1992; Kelso et al. 1991b). If this latter interpretation is the case, then similarities between very diverse forms of behavior, both spatial and temporal may be shown to have very similar dynamical properties. The switching back and forth observed in the data of S5 and S6, although not what we expected, is consistent with previous work on intentional switching in bimanual coordination. Kelso et al. (1988) (see also Scholz and Kelso 1990) demonstrated that patterns of interlimb coordination may be produced at frequencies higher than the typical (spontaneous) switching frequency. That is, conscious effort or intention can stabilize (within limits) otherwise unstable patterns of coordination. In some respects, this is what we observed in the switching behavior of S5 and S6. To explore fully such intentional influences in this task, it will be necessary to examine in detail spatial patterns within an intentional switching paradigm similar to the one devised by Kelso et al. (1988). On the basis of the temporal stability of the spatial patterns various predictions regarding switching time from one pattern to the other can be made and tested.

Three aspects of the results we report here bear directly on previous work focusing on the problem of trajectory formation. First, other authors have emphasized how variability in the end-effector's kinematics varies systematically as a function of the geometry (curvature) of the path (Viviani and Schneider 1991). However, such systematic variation provides no insight into the direction of the pattern change observed here or the lack of specific changes in spatial variability as frequency of motion increased. In fact, a close inspection of the trajectories presented in Fig. 4A and B shows that near points of maximum curvature a decrease in the spatial or geometric variability occurred in both figures. This finding agrees with other observations (Viviani and Schneider 1991), but again does not help in identifying the system's relevant degrees of freedom for the production of such spatial figures. Nor do the slight differences in component displacement lead to any predictions regarding the direction of pattern switching. Rather, as shown here, it is

the temporal patterning of the end-effector's trace (xy) that allows for the identification of the relevant task-specific degrees of freedom. A second issue concerns so-called redundancy, which was minimized in our experiment by limiting the motion in joint space to two degrees of freedom (flexion-extension and abduction-adduction). Thus our system can be described in terms of a one-to-one mapping between joint space and end-effector space. As the results show, the behavior of the end effector in each pattern can be said to approximate sinusoidal motion in the two available spatial degrees of freedom. These results conform to the motion of an end effector in a multijoint limb (Soechting and Terzuolo 1986; Viviani and Schneider 1991). Whether or not excess degrees of freedom exist in joint space, it seems that a main organizational property of the central nervous system is that motion at the end effector approximates sinusoidal motion. Such a phenomenon, however, provides no relevant information regarding the organizational principles that underlie pattern switching, which, as we demonstrate here, is intimately related to pattern stability. The third point speaks to the notion of piecewise planar motion in the end effector. Several researchers (e.g. , Morasso 1983; Soechting and Terzuolo 1987a, b) have noted that three-dimensional trajectories may be described as consisting of planar segments. A segment is defined as that piece of a trajectory that lies on a single plane of motion, e.g., frontal sagittal, oblique. It is hypothesized that the construction of such trajectories consists of planning individual arcs or segments that must be linked together to form the complete trajectory. As before, each segment is constrained to approximate sinusoidal motion in two dimensions. Although our experiment limited motion to a single plane, temporal analysis allowed us to describe the global dynamics of the pattern without having to decompose it and then reassemble it on the basis of certain linear approximations (cf. Morasso and Mussa-Ivaldi 1982; Morasso 1983; Soechting and Terzuolo 1987a, b). In a forthcoming paper (Fuchs et al. in preparation; for preliminary results see Fuchs et al. 1993) we show that a global description of the patterns and pattern switching may be achieved by starting with the assumption of linear sinusoidal motion, and then developing a one-dimensional nonlinear equation of motion based on the amplitudes of the components.

The results we report here suggest that the flexible assembly of spatial patterns of coordination or trajectories takes the form of a *coordination dynamics* (Kelso 1994). In the case presented, these coordination dynamics are defined by the temporal relationship of the spatial components (x, y) of the trajectory and control parameters such as movement rate. Following along these lines, experiments focusing on such spatial transitions in a multijoint system may lead to a better understanding of the mapping between a redundant joint space and the trajectory of an end effector (see e.g., Buchanan et al. 1994).

Acknowledgements. This work was supported by NIMH grant MH42900 and ONR grant N0014-92-J-1904.

References

Abend W, Bizzi E, Morasso P (1982) Human arm trajectory formation. Brain 105:331–348

Atkeson CG, Hollerbach JM (1985) Kinematic features of unrestrained vertical arm movements. J Neurosci 5:2318–2330

Beek PJ (1989) Timing and phase-locking in cascade juggling. Eco Psychol 1:55–96

Beek PJ, Peper CE, Wieringen PCW van (1992) Frequency locking, frequency modulation, and bifurcation in dynamic movement systems. In: Stelmach GE, Requin J (eds) Tutorials in motor behavior, vol 2. North-Holland, Amsterdam, pp 599–622

Bizzi E, Mussa-Ivaldi FA, Giszter S (1991) Computations underlying the execution of movement: a biological perspective. Science 253:287–291

Bizzi E, Hogan N, Mussa-Ivaldi FA, Giszter S (1992) Does the nervous system use equilibrium point control to guide single and multijoint movements. Behav Brain Sci 15:603–631

Buchanan JJ, Kelso JAS (1993) Posturally induced transitions in rhythmic multijoint limb movements. Exp Brain Res 94:131–142

Buchanan JJ, Deguzman GC, Kelso JAS, Treffner PJ (1994) The suppression and activation of degrees of freedom in trajectory formation. In: Proceedings of the 24th Annual Society for Neuroscience Meeting, vol 20, p 544

DeGuzman GC, Kelso JAS (1991) Multifrequency behavioral patterns and the phase attractive circle map. Biol Cybern 64:485–495

DeGuzman GC, Kelso JAS (1992) The flexible dynamics of biological coordination: living in the niche between order and disorder. In: Baskin AB, Mittenthal JE (eds) Principles of organization in organisms. (Proceedings of the Santa Fe Institute, vol 12) Addison-Wesley, Reading, Mass., pp 11–34

Flash T, Hogan N (1985) The coordination of arm movements: an experimentally confirmed mathematical model. J Neurosci 5:1688–1703

Fuchs A, Kelso JAS, Buchanan JJ (1993) Trajectory formation and the coordination dynamics of spatiotemporal patterns. II. Theoretical results. In: Proceedings of the 23rd Annual Society for Neuroscience Meeting, vol 19, p 544

Fuchs A, Kelso JAS, Buchanan JJ (in preparation) Order parameters for the coordination dynamics of trajectory formation.

Greene PH (1982) Problems of organization of motor systems. In: Rosen R, Snell FM (eds) Progress in theoretical biology. Academic Press, New York, pp 303–338

Haken H (1983) Synergetics, an introduction: non-equilibrium phase transitions and self-organization in physics, chemistry and biology. Springer, Berlin Heidelberg New York

Haken H (1987) Information compression in biological systems. Biol Cybern 56:11–17

Haken H (1988) Information and self-organization: a macroscopic approach to complex systems. Springer, Berlin Heidelberg New York

Haken H, Kelso JAS, Bunz H (1985) A theoretical model of phase transitions in human hand movements. Biol Cybern 51: 347–356

Hollerbach JM (1981) An oscillation theory of handwriting. Biol Cybern 39:139–156

Kelso JAS (1981) On the oscillatory basis of movement. Bull Psychon Soc 18:63

Kelso JAS (1984) Phase transitions and critical behavior in human bimanual coordination. Am J Physiol 15:R1000–R1004

Kelso JAS (1990) Phase transitions: foundations of behavior. In: Haken H (ed) Synergetics of cognition. Springer, Berlin Heidelberg New York, pp 249–268

Kelso JAS (1994) Elementary coordination dynamics. In: Swinnen S, Heuer H, Massion J, Casaer P (eds) Interlimb coordination: neural, dynamical and cognitive constraints. Academic Press, New York, pp 301–318

Kelso JAS (1995) Dynamic patterns: the self-organization of brain and behavior. MIT Press, Cambridge, Mass

Kelso JAS, DeGuzman GC (1988) Order in time: how cooperation between the hands informs the design of the brain. In: Haken H (ed) Neural and synergetic computers. Springer, Berlin Heidelberg New York, pp 180–196

Kelso JAS, Scholz JP (1985) Cooperative phenomena in biological motion. In: Haken H (ed) Complex systems: operational approaches in neurobiology, physical systems and computers. Springer, Berlin Heidelberg New York, pp 124–149

Kelso JAS, Schöner G (1987) Toward a physical (synergetic) theory of biological coordination. Springer Proc Phys 19:224–237

Kelso JAS, Southard DL, Goodman D (1979) On the nature of human interlimb coordination. Science 203:1029–1031

Kelso JAS, Scholz JP, Schöner G (1986) Non-equilibrium phase transitions in coordinated biological motion: critical fluctuations. Phys Lett 118A:279–284

Kelso JAS, Scholz JP, Schöner G (1988) Dynamics governs switching among patterns of coordination in biological movement. Phys Lett. 134A:8–12

Kelso JAS, Buchanan JJ, Wallace SA (1991a) Order parameters for the neural organization of single, multijoint limb movement patterns. Exp Brain Res 85:432–444

Kelso JAS, DeGuzman GC, Holroyd T (1991b) Synergetic dynamics of biological coordination with special reference to phase attraction and intermittency. In: Haken H, Köepchen HP (eds) Rhythms in physiological systems. (Springer series in synergetics, vol 55) Springer, Berlin Heidelberg New York, pp 195–213

Kelso JAS, Delcolle JD, Schöner G (1990) Action-perception as a pattern formation process. In Jeannerod M (ed), Attention and performance, vol 13. Erlbaum, Hillsdale, NJ, pp 136–169

Kelso JAS, Buchanan JJ, DeGuzman GC, Ding M (1993) Spontaneous recruitment and annihilation of degrees of freedom in biological coordination. Phys Lett 179A:364–371

Kelso JAS, Buchanan JJ, Murata T (1994) Multifunctionality and switching in the coordination dynamics of reaching and grasping. Hum Mov Sci 13:63–94

Lacquaniti F, Soechting JF (1982) Coordination of arm and wrist motion during a reaching task. Neuroscience 2:399–408

Morasso P (1981) Spatial control of arm movements. Exp Brain Res 42:223–227

Morasso P (1983) Three dimensional arm trajectories. Biol Cybern 48:187–194

Morasso P, Mussa-Ivaldi FA (1982) Trajectory formation and handwriting, a computation model. Biol Cybern 45:131–142

Saltzman EL, Kelso JAS (1987) Skilled actions: a task dynamic approach. Psychol Rev 94:84–106

Schmidt RC, Carello C, Turvey MT (1990) Phase transitions and critical fluctuations in the visual coordination of rhythmic movements between people. J Exp Psychol Hum Percept Perform 16:227–247

Scholz JP, Kelso JAS (1989) A quantitative approach to understanding the formation and change of coordinated movement patterns. J Motor Behav 21:122–144

Scholz JP, Kelso JAS (1990) Intentional switching between patterns of bimanual coordination is dependent on the intrinsic dynamics of the patterns. J Motor Behav 22:98–124

Scholz JP, Kelso JAS, Schöner G (1987) Non-equilibrium phase transitions in coordinated biological motion: critical slowing down and switching time. Phys Lett 123A:390–394

Schöner G, Kelso JAS (1988a) Dynamic pattern generation in behavioral and neutral systems. Science 239:1513–1520

Schöner G, Kelso JAS (1988b) Dynamic patterns in biological coordination: theoretical strategy and new results. In: Kelso JAS, Mandell AJ, Shlesinger MF (eds) Dynamic patterns in complex systems. World Scientific, Singapore, pp 77–102

Schöner G, Haken H, Kelso JAS (1986) A stochastic theory of phase transitions in human hand movement. Biol Cybern 53:442–452

Soechting JF (1989) Elements of coordinated arm movements in three dimensional space. In: Wallace SA (ed) Perspectives on the coordination of movement. Elsevier, Amsterdam, pp 47–83

Soechting JF, Lacquaniti F (1981) Invariant characteristics of a pointing movement in man. Neuroscience 1:710–720

Soechting JF, Terzuolo CA (1986) An algorithm for the generation of curvilinear wrist motion in an arbitrary plane in three-dimensional space. Neuroscience 19:1393–1406

Soechting JF, Terzuolo CA (1987a) Organization of arm movement is segmented. Neuroscience 23:39–52

Soechting JE, Terzuolo CA (1987b) Organization of arm movements in three dimensional space: wrist motion is piecewise planar. Neuroscience 23:53–61

Soechting JF, Terzuolo CA (1990) Sensorimotor transformations and the kinematics of arm movements in 3-d space. In: Jeannerod M (ed) Attention and performance, vol 13. Erlbaum, Hillsdale, NJ, pp 474–494

Soechting JF, Lacquaniti F, Terzuolo CA (1986) Coordination of arm movements in three dimensional space: sensorimotor mapping during drawing movements. Neuroscience 17: 295–311

Treffner PJ, Turvey MT (1993) Resonance constraints on rhythmic movements. J Exp Psychol Hum Percept Perform 9: 1221–1237

Uno Y, Kawato M, Suzuki R (1989) Formation and control of optimal trajectory in human multijoint arm movement. Biol Cybern 61:89–101

Viviani P, Schneider R (1991) A developmental study of the relationship between geometry and kinematics in drawing movements. J Exp Psychol Hum Percept Perform 17:198–218

Wimmers RH, Beek PJ, Wieringen PCW van (1992) Phase transitions in rhythmic tracking movements: a case of unilateral coupling. Hum Mov Sci 11:217–226